Assessing middle atmosphere weather models using LiDAR and ambient noise: a case study for IS26

Patrick Hupe[1], Lars Ceranna[1], Christoph Pilger[1], Marine de Carlo[2], Alexis Le Pichon[2], Bernd Kaifler[3], Markus Rapp[3,4]

[1] BGR/B4.3, Hannover, Germany
[2] CEA/DAM/DIF, Arpajon, France
[3] DLR/IPA, Oberpfaffenhofen, Germany
[4] LMU/MIM, Munich, Germany

SnT2019, T1.1-O2
25 June 2019

ARISE
Atmospheric dynamics Research InfraStructure in Europe

BGR Bundesanstalt für Geowissenschaften und Rohstoffe

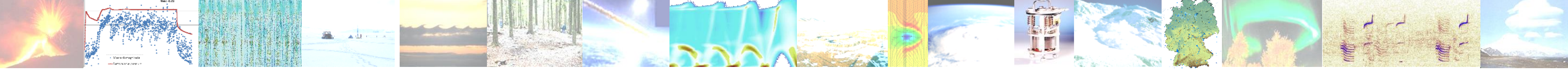

Fluctuations in the direction and amplitude of microbarom detections

- Microbaroms produce false alarms in routine infrasound processing (e.g., Arrowsmith, 2018)
- Microbaroms provide information on the middle-atmosphere dynamics (e.g., Landès et al., 2014; Smets & Evers, 2014)

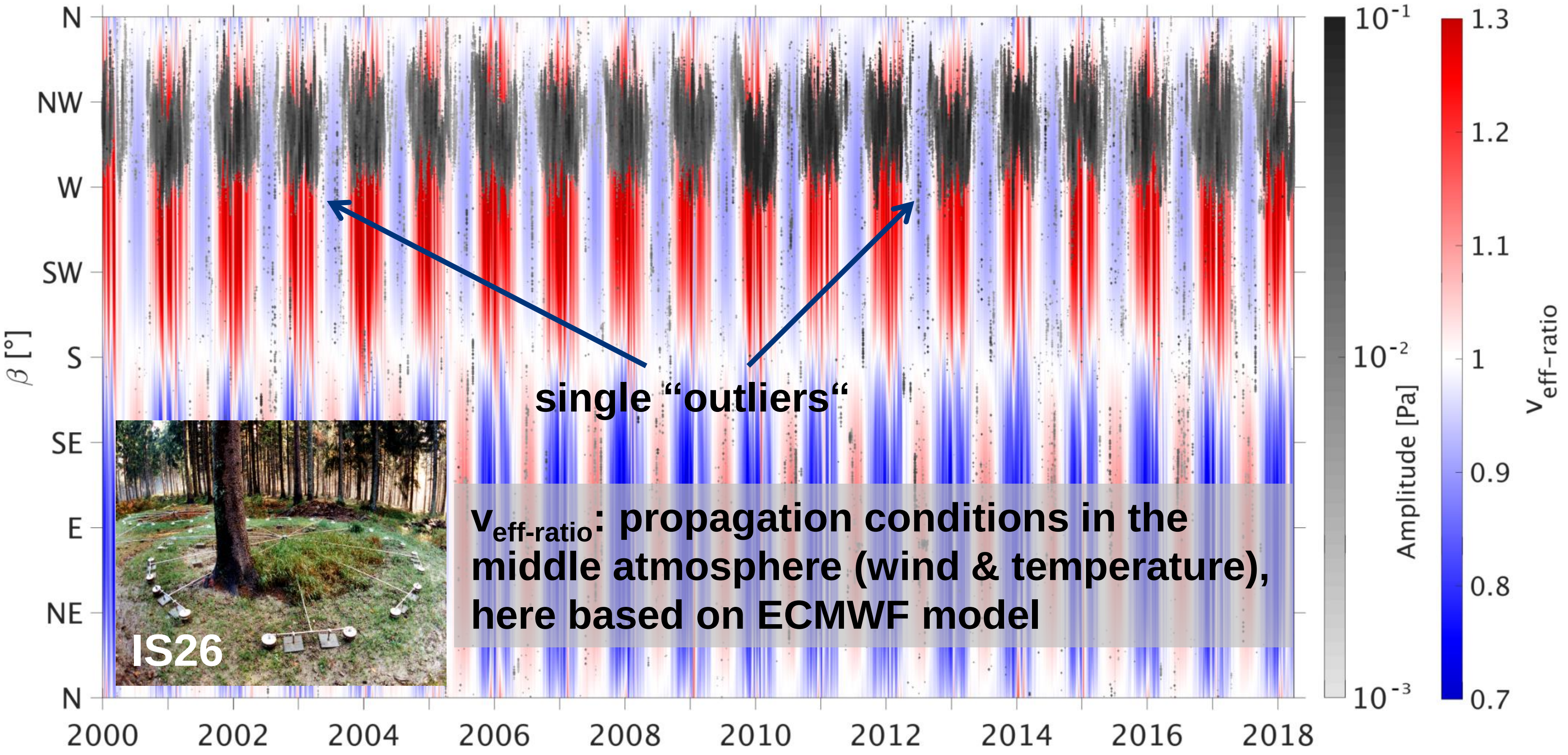

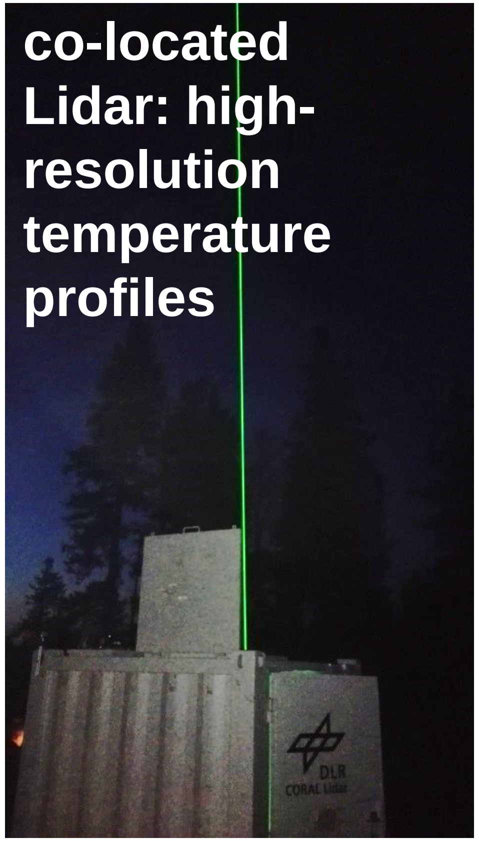

Outline

Data, methodology and modeling scheme

Microbarom modeling at IS26, relying on the ECMWF atmospheric analysis

Uncertainty inferred from the representation of middle atmosphere dynamics in weather models

Results of the amplitude (uncertainty) modeling

Conclusions & perspectives

BGR Bundesanstalt für Geowissenschaften und Rohstoffe

Data, methodology and modeling scheme

ECMWF ([u,v], T)

atmospheric propagation

Lidar (T)

[u,v], T uncertainty

source model (ocean swell)

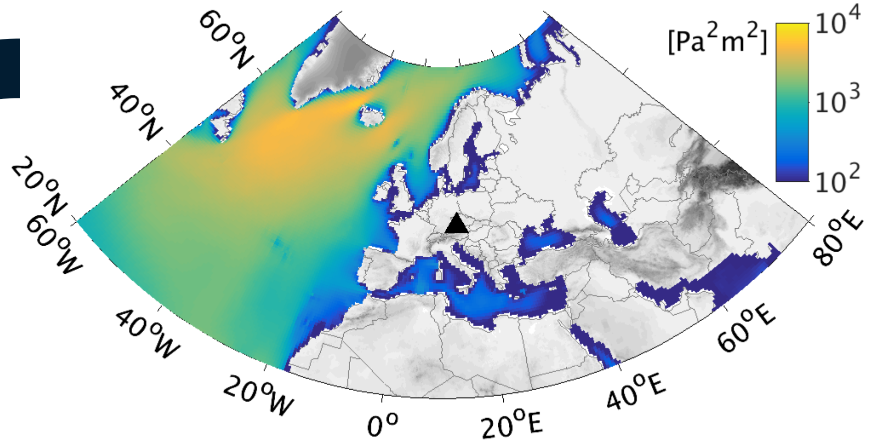

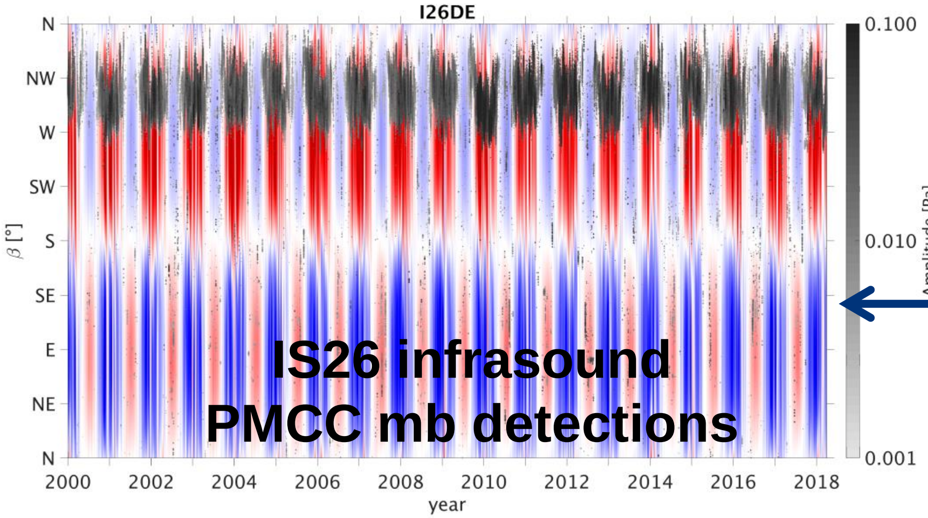

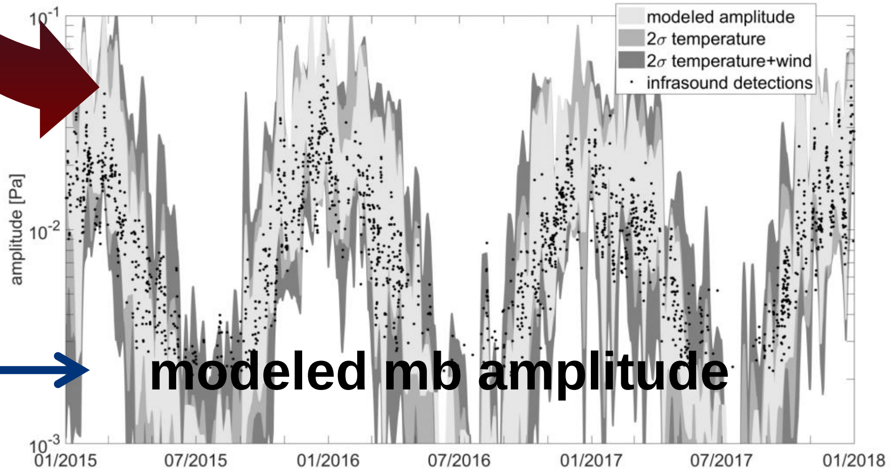

Bundesanstalt für Geowissenschaften und Rohstoffe

Data, methodology and modeling scheme

ECMWF ([u,v], T) → **atmospheric propagation**

$$A_p(f, r, v_{eff-ratio}) = \frac{1}{r} 10^{\frac{a(f)\,r}{20}} + \frac{r^{b(f, v_{eff-ratio})}}{1 + 10^{\frac{d-r}{s(f)}}}$$

High-resolution operational atmospheric analysis by the Integrated Forecast System of the European Centre for Medium-Range Weather Forecasts (ECMWF)

- Resolution: 0.5° x 0.5°, 6 h
- 137 model levels (0–78 km)
- Sponge layers above 45 km for damping wave reflections

Semi-empirical attenuation relation (Le Pichon et al., 2012)

- Parameters a, b, d, and s describe near- and far-field dissipation of waves
- Parameters depend on effective sound speed ratio

$$v_{eff} = c_T + w_\alpha \approx 20.05\sqrt{T} + w_\alpha \quad (\text{in m s}^{-1})$$

$$v_{eff-ratio} = \frac{v_{eff,z}}{v_{eff,z0}}$$: max(40 km ≤ z < 60 km)

Data, methodology and modeling scheme

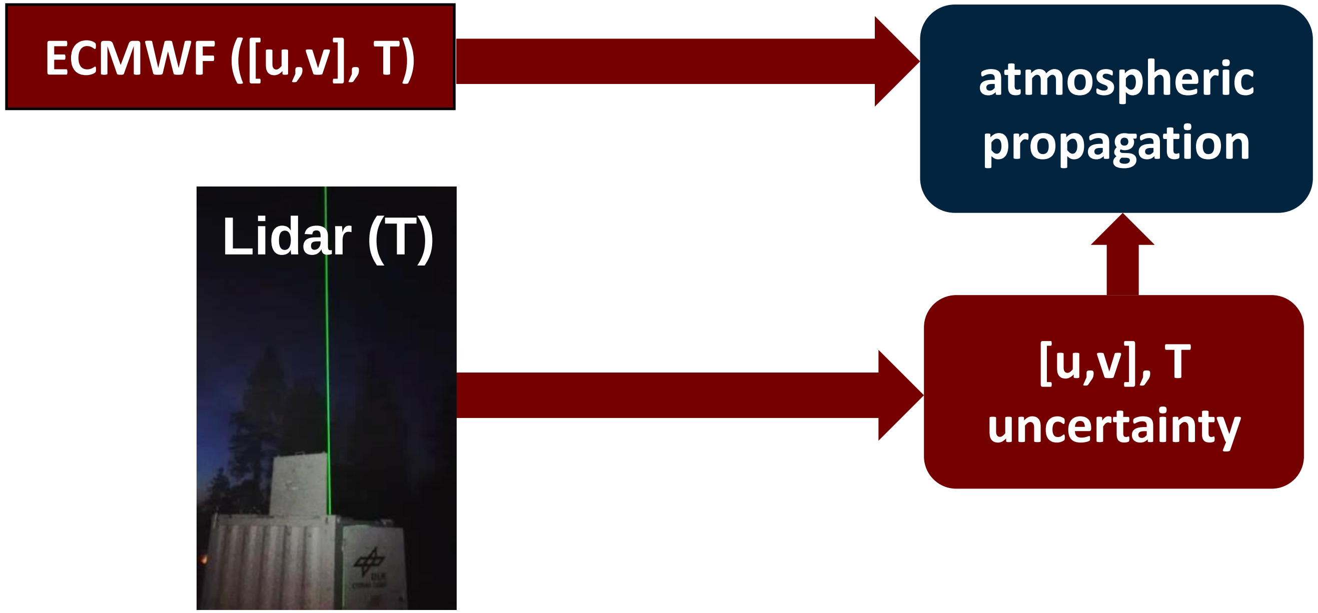

$$A_p(f, r, v_{eff-ratio}) = \frac{1}{r} 10^{\frac{a(f)\, r}{20}} + \frac{r^{b(f, v_{eff-ratio})}}{1 + 10^{\frac{d-r}{s(f)}}}$$

$$v_{eff} = c_T + w_\alpha \approx 20.05 \sqrt{T} + w_\alpha \quad (\text{in m s}^{-1})$$

$$v_{eff-ratio} = \frac{v_{eff,z}}{v_{eff,z0}}$$

Compact Rayleigh Autonomous Lidar (CORAL)

T1.1-P10

- (Laser-)light detection and ranging
- Vertical profiles of the temperature (density)
- Resolution: 1 km in the vertical, 10 min integration time
- Co-located to IS26 from May to Nov 2016 (ARISE-2 project)

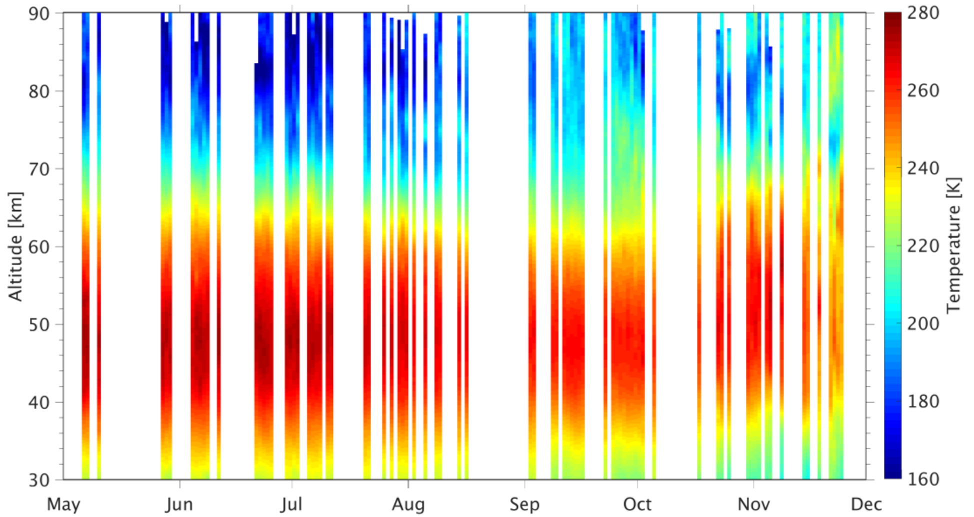

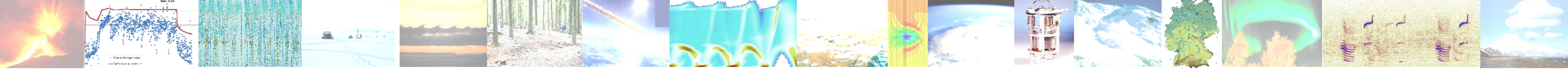

Data, methodology and modeling scheme

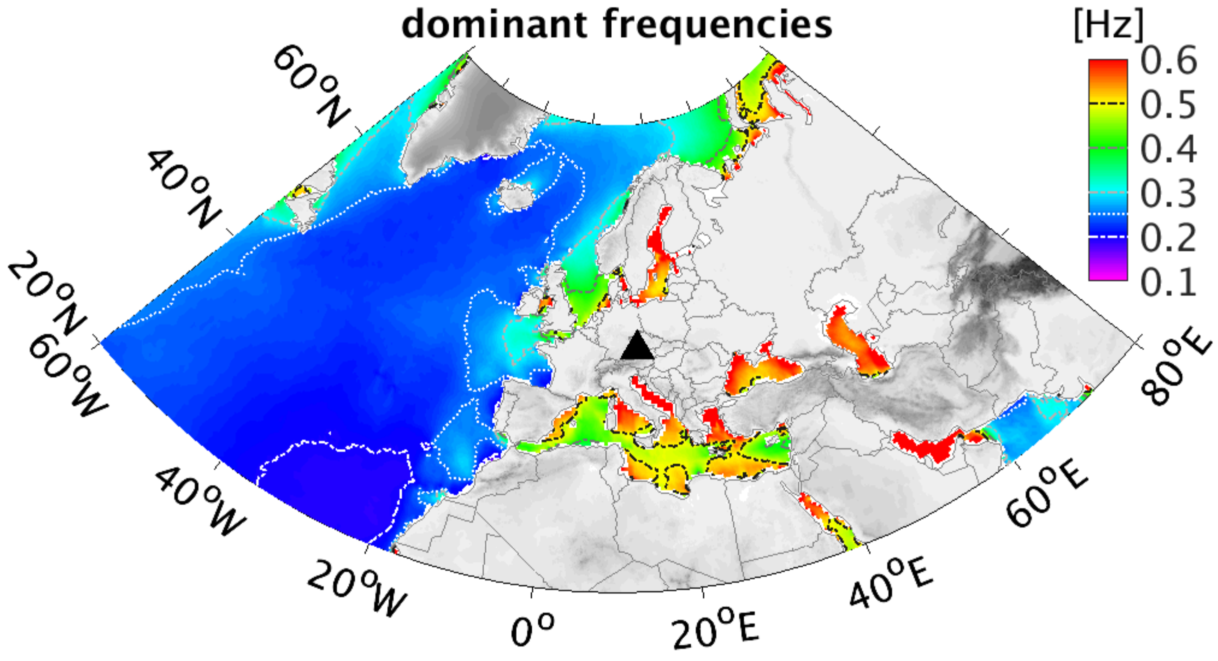

Data source: IFREMER, Ardhuin et al. 2011

source model (ocean swell)

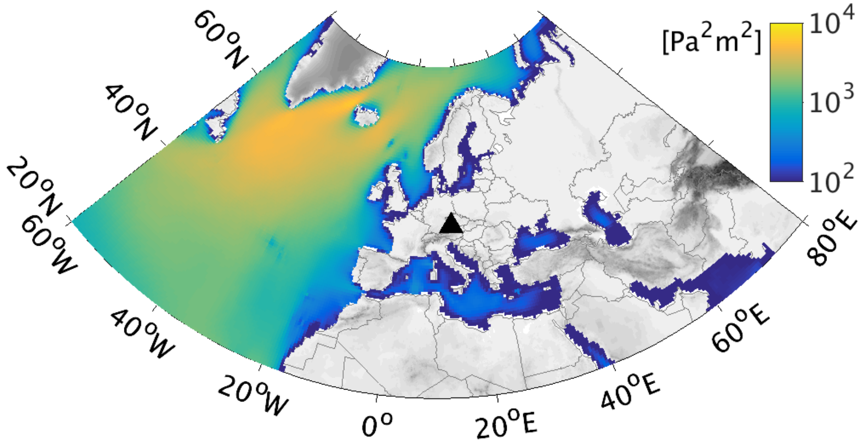

- based on WaveWatch III (NASA) and ECMWF's high-resolution analysis winds
- Resolution: 0.5° x 0.5°, 3 h
- Daily & seasonal variation in acoustic source pressure
- Strongest sources on the open ocean
- Peak frequencies around 0.25 Hz

Data, methodology and modeling scheme

ECMWF ([u,v], T)

atmospheric propagation

[u,v], T uncertainty

source model (ocean swell)

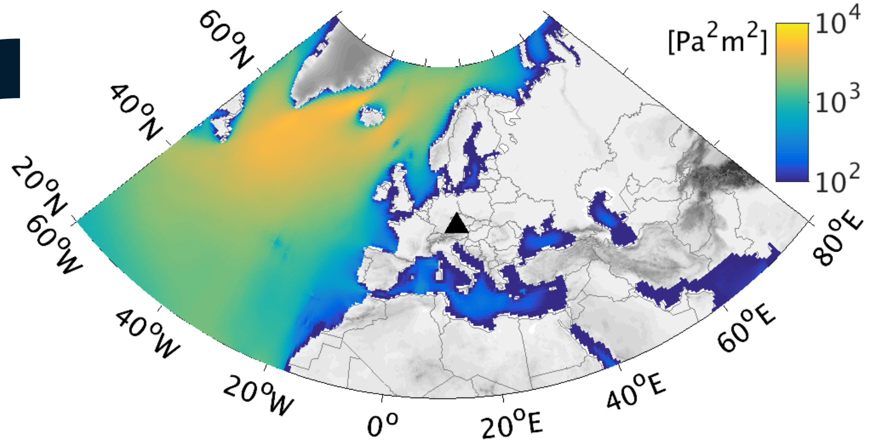

modeled mb amplitude

Assumption (1)
Homogeneous conditions along the propagation path (ECMWF profiles at IS26)

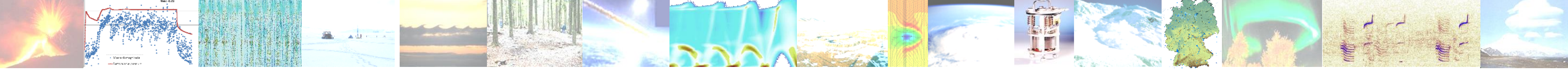

Microbarom modeling at IS26, relying on the ECMWF atmospheric analysis

Acoustic source pressure | **Integrated attenuation**

July

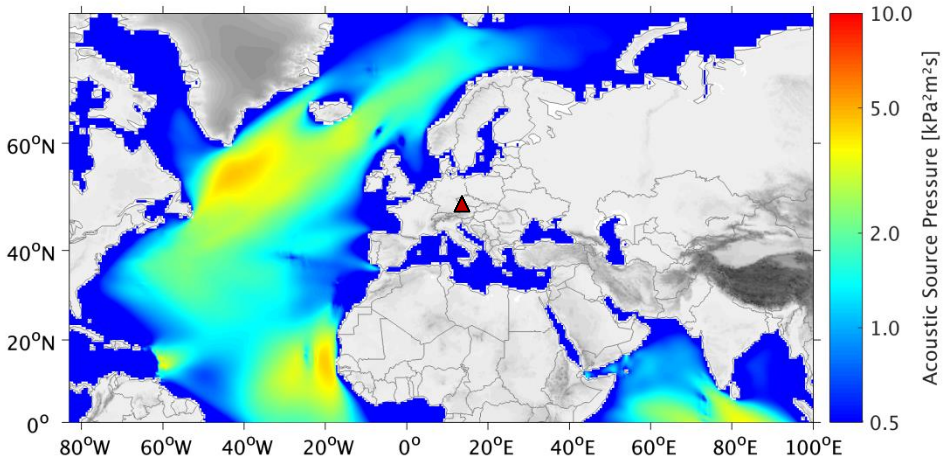

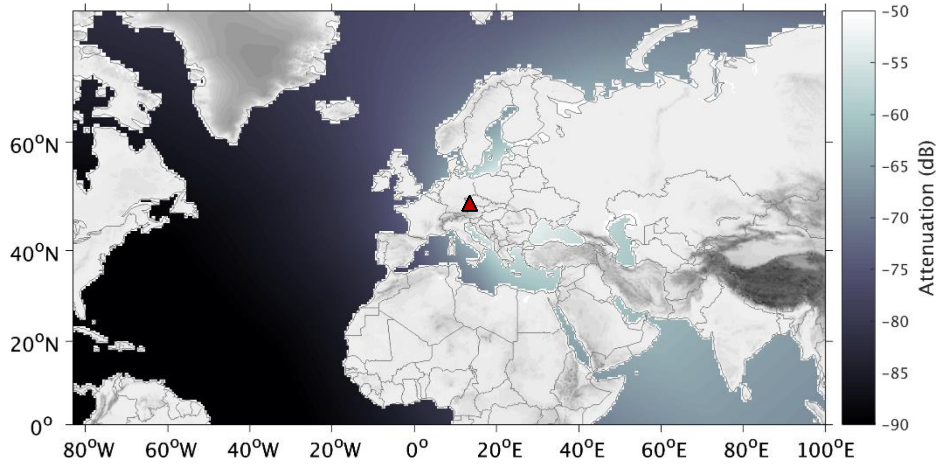

November

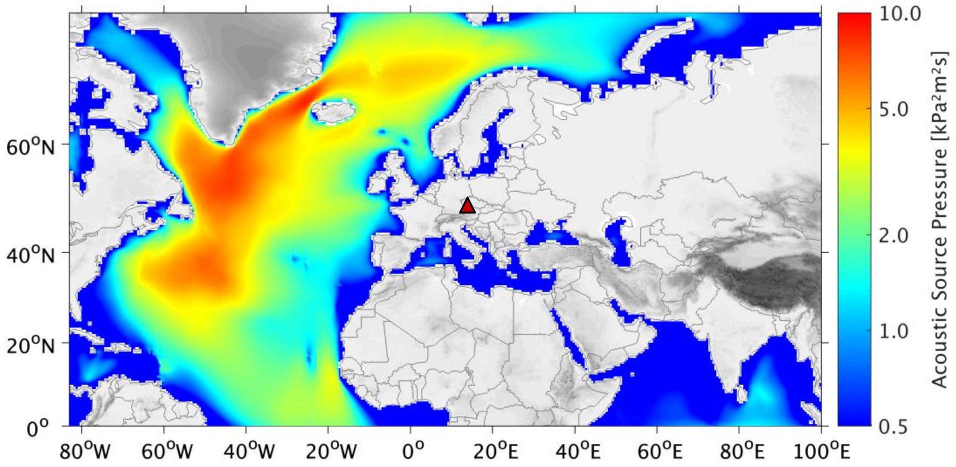

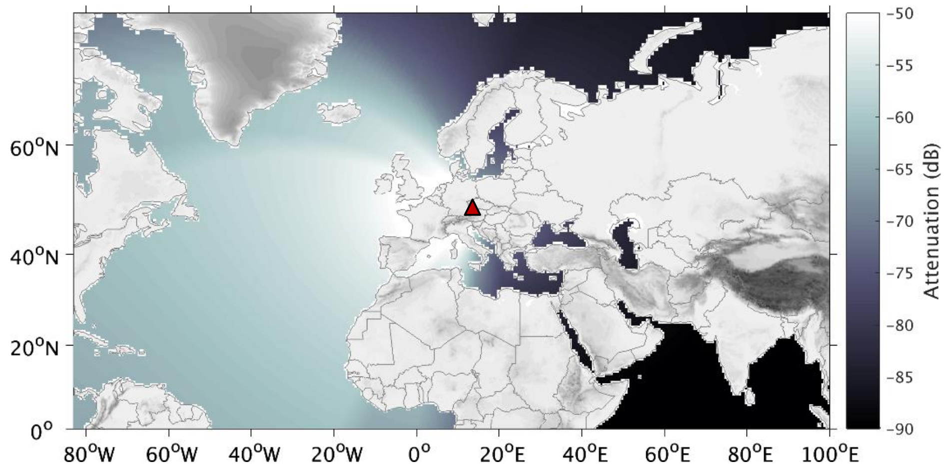

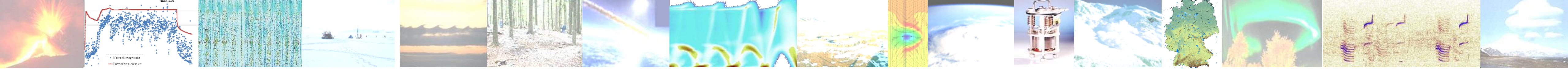

Microbarom modeling at IS26, relying on the ECMWF atmospheric analysis

Acoustic source pressure | Predicted amplitude at IS26

July

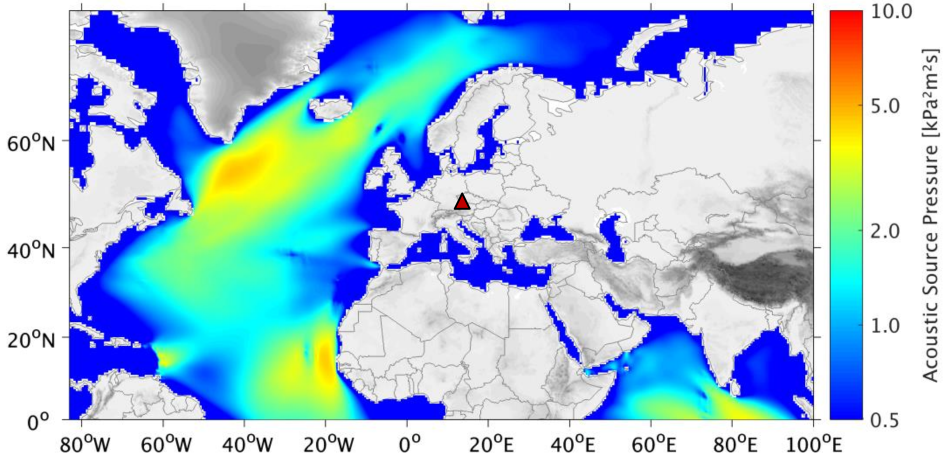

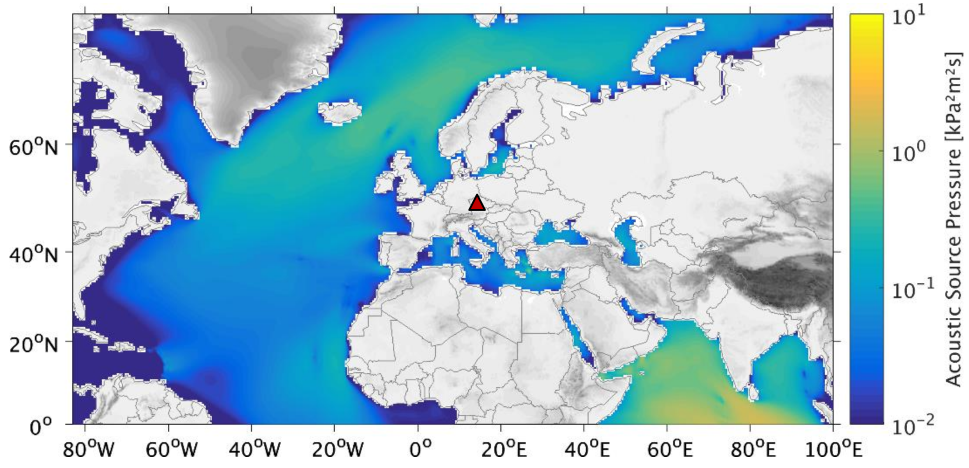

November

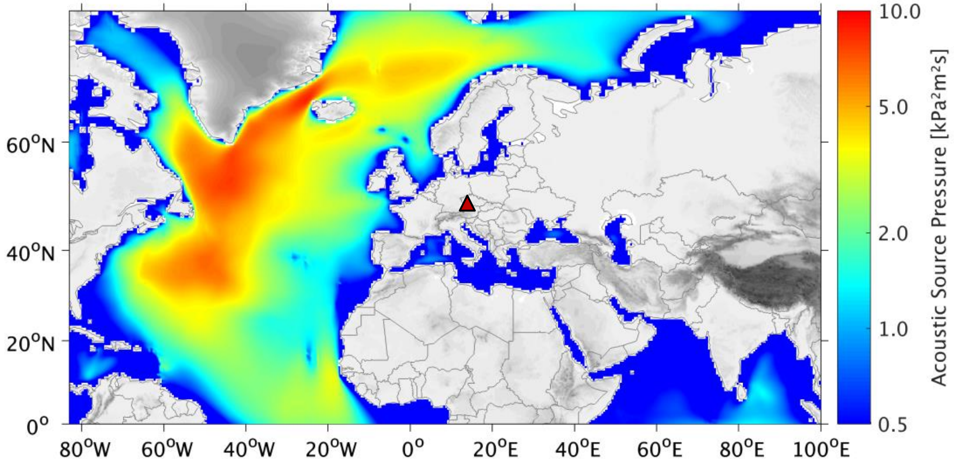

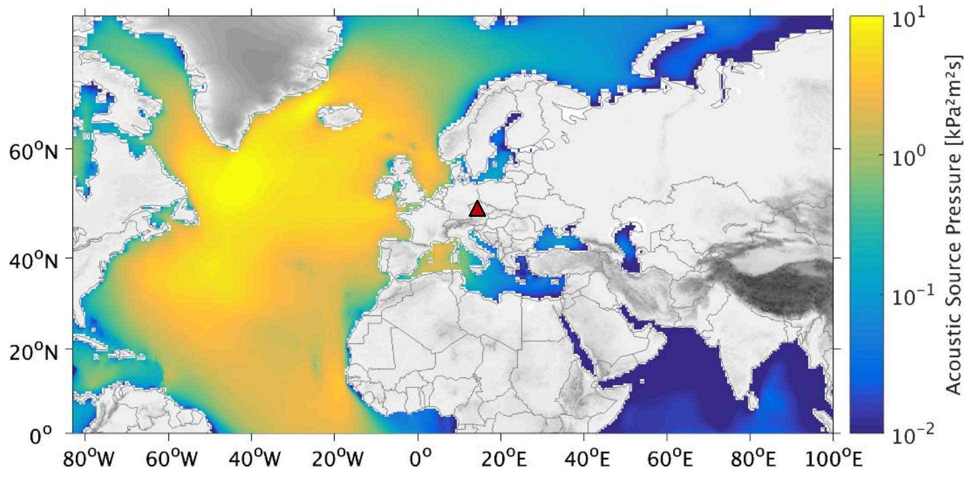

Microbarom modeling at IS26, relying on the ECMWF atmospheric analysis

Modeled period: 2015–2017

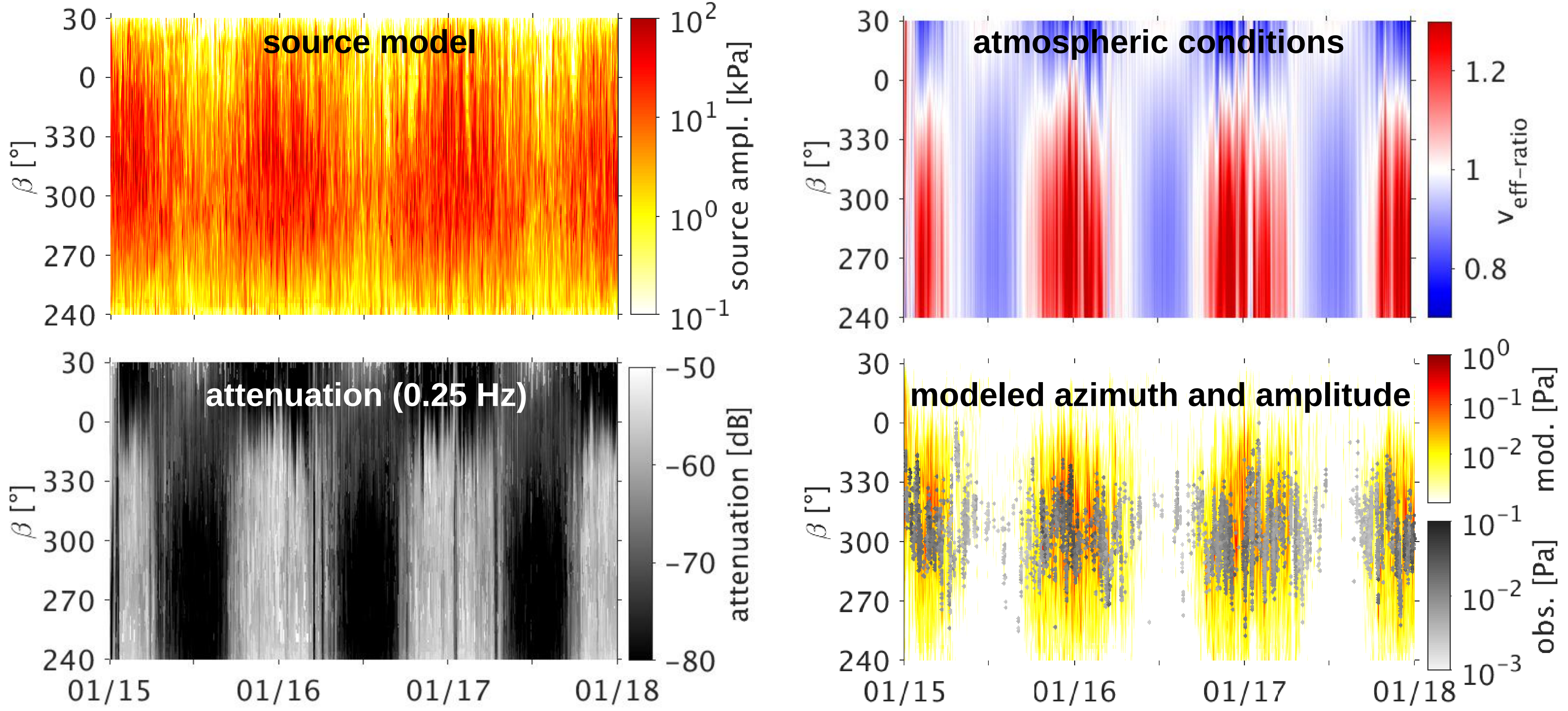

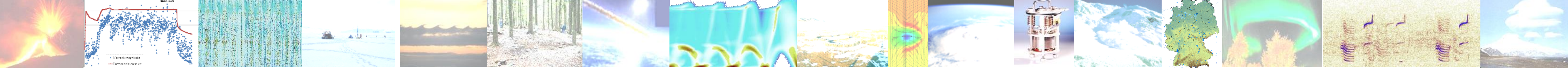

Uncertainty inferred from the representation of middle atmosphere dynamics in weather models

Temperature bias in ECMWF analysis

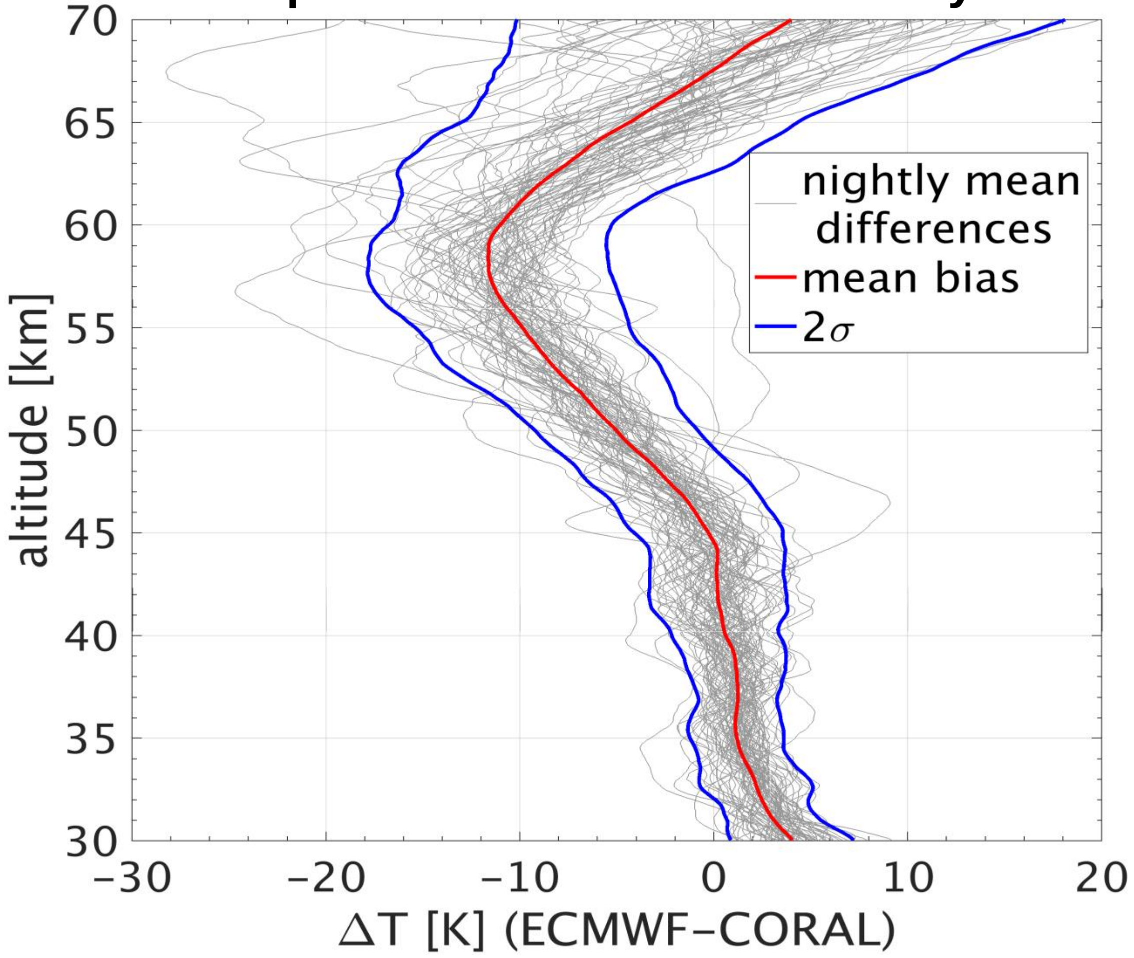

Temperature data: mobile CORAL lidar, Germany (2016)
Wind data: ALOMAR RMR lidar, Norway (2016) – **assumption (2)**

Each 100 perturbations of [u,v] and T (effective sound speed), based on observations (2σ range)

→ Resulting amplitude range reflects uncertainty inferred from NWP models

Results of the amplitude (uncertainty) modeling

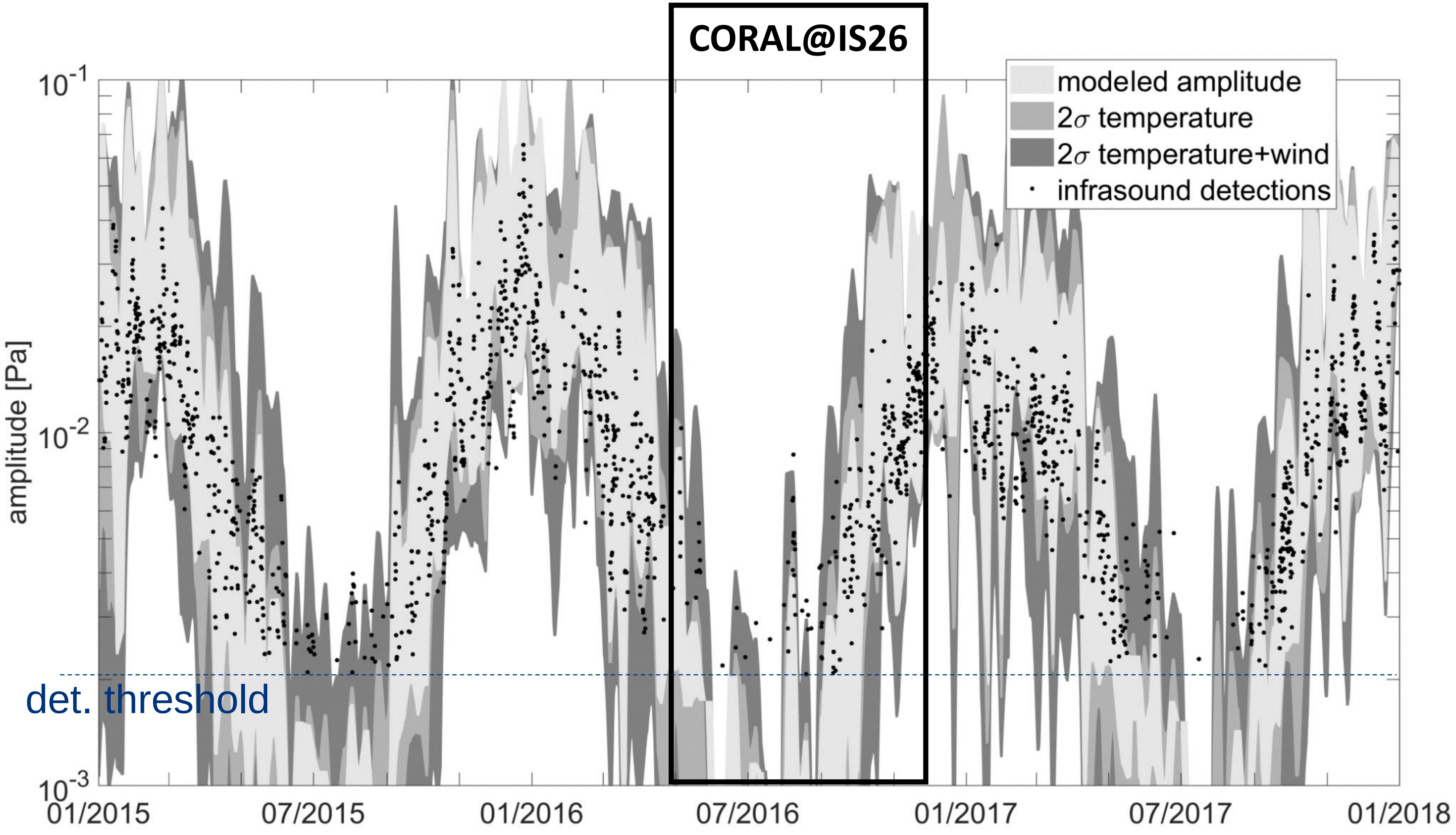

"amplitude range": 2d-variability of ocean swell sources, based on ECMWF

Dominant PMCC detections within Δt = 3 h

Microbarom modeling scores (PMCC detections within amplitude range):

ECMWF only – 77%
ECMWF+ΔT (Lidar) – 86%
ECMWF+ΔT+Δ[u,v] – 97%

Maximum improvement in the summer (+58%)

Conclusion & perspectives

- Atmospheric uncertainties in the temperature and winds have an operational impact for IDC/NDCs in terms of explaining “false alarms“
- Continuous microbarom observations are useful for assessing (and improving) the accuracy of the middle atmosphere circulation in numerical weather prediction models
- Co-located infrasound and lidar: better understanding of the variations in microbarom detections
- The impact of winds is more significant than that of the temperature
- **Need for vertical profiles of the horizontal wind vector – i.e., development of a mobile wind lidar**
- **Increase the duration of co-located measurements (e.g., at IS02 – poster T1.1-P6)**
- **Incorporate data of additional instruments (e.g., wind radiometers)**
- **ARISE follow-up: pilot station at IS26 for additional co-located technologies**
- **Equipping multiple IMS infrasound stations with lidars? – from local to global studies!**

Thank you!

Hupe, P., L. Ceranna, C. Pilger, M. De Carlo, A. Le Pichon, B. Kaifler, and M. Rapp (2019) Assessing middle atmosphere weather models using infrasound detections from microbaroms. *Geophys. J. Int.*, **216**(3), 1761–1767, doi:10.1093/gji/ggy520.

Related posters:

T1.1-P6	**a related study at IS02 using one year of lidar data**
T1.1-P8	**global microbarom observations and modeling**
T1.1-P10	**the lidar CORAL & gravity wave observations at IS02**

Bibliography

Ardhuin, F., E. Stutzmann, M. Schimmel, and A. Mangeney (2011) Ocean wave sources of seismic noise. *J. Geophys. Res.*, **116**, C09004, doi:10.1029/2011JC006952.

Arrowsmith, S. J. (2018) False alarms and the IMS infrasound network: understanding the factors influencing the creation of false events. *Geophys. J. Int.*, **215**(2), 1322–1337, doi:10.1093/gji/ggy350.

Landès, M., A. Le Pichon, N. M. Shapiro, G. Hillers, and M. Campillo (2014) Explaining global patterns of microbarom observations with wave action models. *Geophys. J. Int.*, **199**(3), 1328–1337, doi:10.1093/gji/ggu324.

Le Pichon, A., L. Ceranna, and J. Vergoz (2012) Incorporating numerical modeling into estimates of the detection capability of the IMS infrasound network. *J. Geophys. Res.*, **117**, D05121, doi:10.1029/2011JD016670.

Smets, P. S. M. and L. G. Evers (2014) The life cycle of a sudden stratospheric warming from infrasonic ambient noise observations. *J. Geophys. Res.*, **119**(21), 12084–12099, doi:10.1002/2014JD021905.